Josephson-Junction Mixer Analysis Using Frequency-Conversion and Noise-Correlation Matrices

YUAN TAUR

Abstract—A complete characterization and optimization have been carried out for an externally pumped Josephson-junction mixer. A noise-driven nonlinear pump equation is first solved in the time domain on a computer in order to obtain a conversion matrix and noise-correlation matrix for the small-signal current and voltage. A set of linear circuit equations formed by the matrices is then solved in the frequency domain for the mixer noise temperature and conversion efficiency. Finally, optimization is made with respect to circuit, bias, and junction parameters to find the ultimate theoretical performance.

I. Introduction

RECENT experimental work has shown that point-contact Josephson junctions can make low-noise millimeter-wave mixers with high conversion efficiency (or gain) [1]-[3]. However, the observed noise is usually one to two orders of magnitude larger than thermal noise at the bath temperature. Although the excess noise has been attributed to a nonlinear process [4], [5], the conversion and noise correlation characteristics of a Josephson mixer are still not well understood quantitatively. This is partly because the nonlinear Josephson equations are difficult to analyze in the case of mixing. In addition, the high-order effect of noise in the junction plays such an important role that the nonlinear equation must be solved with a fluctuating term for thermal noise. This is in contrast to a classical mixer analysis [6] in which noise is simply treated as a small signal.

The first computer calculation on a Josephson mixer by Auracher and Van Duzer [7] predicted conversion gain from the modulation of I-V curve by an RF signal. However, the analysis was carried out for a current source configuration without a treatment of the nonlinear interactions between the mixer and its RF circuit. A subsequent generalization of the calculation [8] took the finite RF source impedance into account to arrive at coupling figures for conversion efficiency. But the approach lacked a noise analysis and was limited only to broad-band resistive circuits. A better understanding of the Josephson mixer was obtained from an electronic analog computer which modeled the narrow-band RF circuit more realistically [9], [10]. With a proper simulation of thermal noise, the analog computer can be used to evaluate mixer noise temperature given a set of parameters. However, analog simulation is inherently limited to one special case at a time, making it very tedious to cover all the parameter values of interest. Moreover, since a general formulation does not exist for the nonlinear conversion process, a systematic search for the optimum condition cannot be carried out.

In this paper, we present a complete analysis to evaluate and optimize the noise temperature of a Josephson-junction mixer. The nonlinear Josephson equation, including both a large RF drive and a noise term, is first solved in the time domain using a digital computer. The results along with their fluctuations can be used to derive a small-signal impedance matrix and a noise-correlation matrix in the frequency domain. Following a general mixer analysis, we then solve a linear circuit equation for conversion efficiency and noise temperature to find out the optimum RF impedance. In this method, all the effects of up-conversion, image-conversion, and noise interaction are included. Furthermore, the advantage of image rejection (single-sideband mixer) can be easily investigated in the frequency-domain analysis. The computation is carried out for a variety of junction and bias parameters to determine the ultimate performance limits of the Josephson mixer.

II. Circuit Model

Since the experimental I-V curves of a low-capacitance point-contact Josephson junction are best described by the resistively shunted junction (RSJ) model [11], this formalism is used in our mixer analysis. In the RSJ model, a resistor of constant resistance R accounts for the quasi-particle current, and is in parallel with an ideal Josephson element which accounts for the superconducting pair current, as shown in the box of Fig. 1. The electrical characteristics of an ideal Josephson element are described by the Josephson relations [12]

$$I_J(t) = I_c \sin \phi(t) \tag{1}$$

$$V(t) = \frac{\hbar}{2e} \frac{d}{dt} \phi(t). \tag{2}$$

Here $\phi(t)$ is the superconducting phase difference across the junction, and I_c is a constant equal to the maximum supercurrent of the junction. Also shown in Fig. 1 is a current source representing Johnson noise having an autocorrelation function

$$\langle \delta I_n(t) \delta I_n(t') \rangle = \frac{2kT}{R} \delta(t - t') \tag{3}$$

Manuscript received February 21, 1980; revised April 18, 1980. This work was supported in part by Columbia Radiation Laboratory, Columbia University, New York, NY, and by Rockwell International Science Center, Thousand Oaks, CA.

The author was with NASA Goddard Institute for Space Studies, Goddard Space Flight Center, New York, NY 10025. He is now with Rockwell International Science Center, Thousand Oaks, CA 91360.

0018/9383/80/1000-1921$00.75

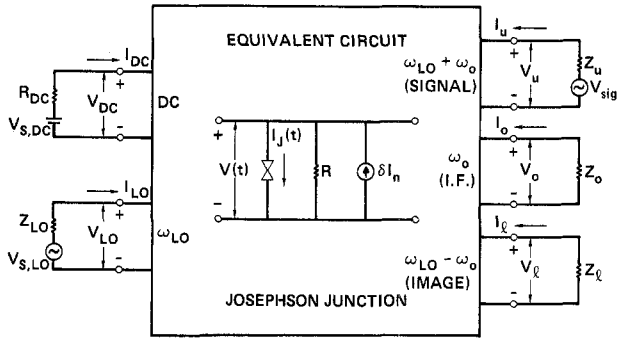

Fig. 1. Equivalent circuit of a Josephson-junction mixer with large-signal sources to the left and small-signal circuits to the right of the junction box. All the external circuits are assumed to be connected to the junction terminals but at different frequencies. The ac current and voltage are expressed in complex half amplitudes.

where T is the ambient temperature. Such a noise term must be included in the nonlinear pump equation as thermal noise cannot be regarded as a small signal.

If the junction is driven by a dc source and a local oscillator (LO) at frequency ω_{LO} as shown to the left of Fig. 1, the pump equation can be written in time domain as

$$\frac{\hbar}{2eR}\frac{d}{dt}\phi(t) + I_c \sin\phi(t) = I_{dc} + (I_{LO}e^{j\omega_{LO}t} + I_{LO}^{*}e^{-j\omega_{LO}t}) + \delta I_n(t). \tag{4}$$

Here we use a complex notation for all ac amplitudes such as $\{V_{S,LO}\exp(j\omega_{LO}t) + V_{S,LO}^{*}\exp(-j\omega_{LO}t)\}$ for the LO generator voltage, and $\{I_{LO}\exp(j\omega_{LO}t) + I_{LO}^{*}\exp(-j\omega_{LO}t)\}$ for the LO current, etc. Equation (4) is valid under the assumption that the embedding circuit has a very high impedance at all frequencies except near dc and ω_{LO}, so that no external current can be generated at the harmonics of the LO frequency: $2\omega_{LO}, 3\omega_{LO}, 4\omega_{LO}, \cdots$, etc. This assumption has been verified from measurements on a scaled point-contact mixer model [13]. However, the impedance of the LO source is finite, which implies that the LO drive is not a constant current source. For a given $V_{S,LO}$, the magnitude of I_{LO} changes with dc bias, and the static I-V curve deviates significantly from that previously published for a constant current source [11].

One can choose a time origin such that I_{LO} is real, and express (4) in terms of dimensionless variables as follows:

$$\frac{d}{d\tau}\phi(\tau) + \sin\phi(\tau) = i_{dc} + 2i_{LO}\cos\Omega_{LO}\tau + \delta i_n(\tau) \tag{5}$$

where $i_{dc} = I_{dc}/I_c$, $i_{LO} = I_{LO}/I_c$, and $\delta i_n = \delta I_n/I_c$ are normalized currents; $\tau = (2eRI_c/\hbar)t$ is normalized time; and $\Omega_{LO} = \hbar\omega_{LO}/2eRI_c$ is normalized LO frequency. A factor of two arises in the LO current due to the half-amplitude notation used here. The noise relationship becomes

$$\langle\delta i_n(\tau)\delta i_n(\tau')\rangle = 2\Gamma\delta(\tau - \tau') \tag{6}$$

where $\Gamma = 2ekT/\hbar I_c$ is a dimensionless noise parameter, equal to the thermal energy kT divided by the Josephson coupling energy $\hbar I_c/2e$. In dimensionless units, the junction is characterized by the parameters Ω_{LO} and Γ; while the bias conditions are represented by the parameters i_{dc} and i_{LO}. Both Ω_{LO} and Γ are important factors governing the mixer performance. It is desirable to keep $\Omega_{LO} < 1$ since most of the RF current would then interact with the inductive Josephson element. The condition $\Gamma < 1$ should also be satisfied, otherwise the Josephson nonlinearity would be smeared out by noise saturation. The region of interest in our analysis is, therefore, restricted to $\Omega_{LO} < 1$ and $\Gamma < 1$, which are satisfied in most experimental situations.

III. Method of Computation and I-V Curves

Given a junction and its bias, the pump equation (5) can be solved numerically for $\phi(\tau)$ on a digital computer (IBM 360/95). A good choice for the integration step is $H = \Delta\tau = 0.25$. No discrepancy is found on a numerical test at half the step size. The noise $\delta i_n(\tau)$ is generated by calling a Gaussian-distributed (approximately) random number at each step of integration. The random numbers have a zero mean and a variance

$$\sigma^2 = 2\Gamma/H \tag{7}$$

depending on the step size. Due to discrete sampling, their spectrum is frequency independent (white) only below $\Omega_n \approx \pi/H(\gg 1)$. However, the junction noise beyond the cutoff does not have any significant effect on the mixer behavior, as has been confirmed in the half-step test.

The normalized junction voltage $v(\tau) = V(t)/RI_c = d\phi(\tau)/d\tau$ can be evaluated once ϕ is solved as a function of τ. It can be expressed in the frequency domain by taking a Fourier transform over a period P equal to ten LO cycles, i.e., $P = 10(2\pi/\Omega_{LO})$

$$v(\tau) = v_{dc} + (v_{LO}e^{j\Omega_{LO}\tau} + v_{LO}^{*}e^{-j\Omega_{LO}\tau}) + (\text{higher frequency components}) \tag{8}$$

where $v_{dc} = V_{dc}/RI_c$ is real but $v_{LO} = V_{LO}/RI_c$ is complex because there is a phase difference between V_{LO} and I_{LO}. Voltage components at harmonic frequencies can be ignored since they do not induce external currents. Both v_{dc} and v_{LO} contain fluctuations due to the noise at low frequency and Ω_{LO}

$$v_{dc} = \langle v_{dc}\rangle + \delta v_{dc} \tag{9}$$

$$v_{LO} = \langle v_{LO}\rangle + \delta v_{LO}. \tag{10}$$

In order to obtain the average as well as the spectral density of fluctuation, the Fourier transform is repeated to yield $v_{dc}^{(1)}, v_{LO}^{(1)}; v_{dc}^{(2)}, v_{LO}^{(2)}; v_{dc}^{(3)}, v_{LO}^{(3)}; \cdots; v_{dc}^{(K)}, v_{LO}^{(K)}$. Therefore, the total period of integration is KP, where $K = 1000$ for an accuracy better than 5 percent. Then the auto- and crosscorrelations can be evaluated as follows:

$$\langle v_{dc}\rangle = \frac{1}{K}\sum_{i=1}^{K} v_{dc}^{(i)} \tag{11}$$

$$\langle v_{LO}\rangle = \frac{1}{K}\sum_{i=1}^{K} v_{LO}^{(i)} \tag{12}$$

$$\langle(\delta v_{dc})^2\rangle_P = \frac{1}{K}\sum_{i=1}^{K} (v_{dc}^{(i)})^2 - \langle v_{dc}\rangle^2 \tag{13}$$

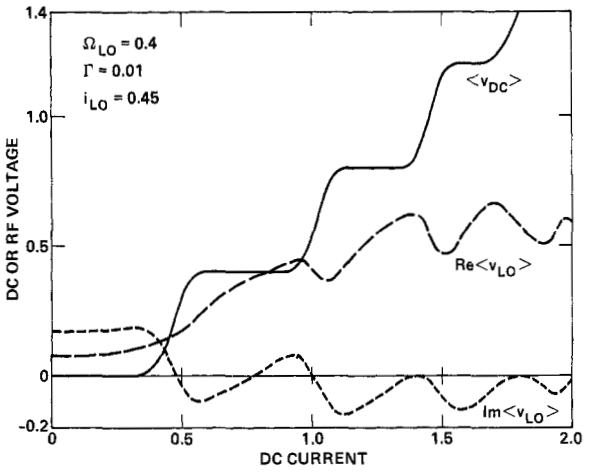

Fig. 2. Normalized dc voltage and in-phase/out-of-phase RF voltages versus dc current (normalized). One expects $\mathrm{Re}\,\langle v_{LO}\rangle \to i_{LO}$ and $\mathrm{Im}\,\langle v_{LO}\rangle \to 0$ at very large dc bias.

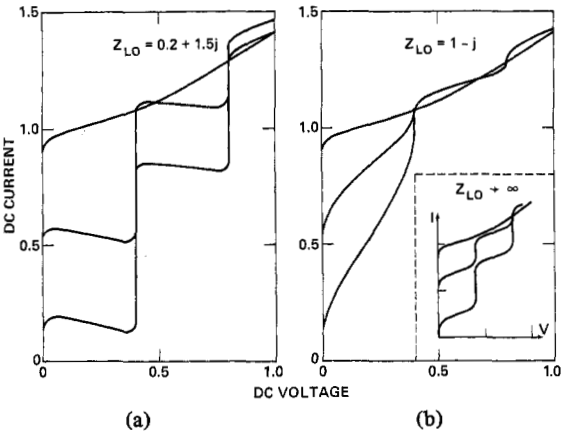

Fig. 3. Two series of I-V curves computed at $\Omega_{LO} = 0.4$ and $\Gamma = 0.01$ for different LO impedances (normalized) shown. In each case, the LO power is zero for the top curve, then increases toward lower curves. The inset shows the case of constant LO current for comparison.

$$\langle |\delta v_{LO}|^2 \rangle_P = \frac{1}{K} \sum_{i=1}^{K} |v_{LO}^{(i)}|^2 - |\langle v_{LO} \rangle|^2 \tag{14}$$

$$\langle (\delta v_{LO})^2 \rangle_P = \frac{1}{K} \sum_{i=1}^{K} (v_{LO}^{(i)})^2 - \langle v_{LO} \rangle^2 \tag{15}$$

$$\langle (\delta v_{dc})(\delta v_{LO}) \rangle_P = \frac{1}{K} \sum_{i=1}^{K} v_{dc}^{(i)} v_{LO}^{(i)} - \langle v_{dc} \rangle \langle v_{LO} \rangle. \tag{16}$$

Here (12), (15), (16) are complex. The subscript P indicates that the correlations depend on the period of Fourier transformation ($\infty 1/P$). These quantities are the ones needed for the mixer noise analysis.

For a given junction and LO frequency, $\langle v_{dc} \rangle$ and $\langle v_{LO} \rangle$ are functions of bias currents i_{dc}, i_{LO}. The dependence on dc bias is shown in Fig. 2, where the quasi-periodic variation is a result of RF-induced Josephson steps. It is found that the out-of-phase RF voltage or $\mathrm{Im}\,\langle v_{LO} \rangle$ does not vanish between steps, which differs from previously computed results in the absence of noise [14]. In fact, it changes from inductive to capacitive as the bias is increased from the first step to the second. This is due to noise rounding or partial RF synchronization of the ac Josephson current off the steps. Another related result is that the noise correlation of the dc and out-of-phase RF voltage or $\mathrm{Im}\,\langle (\delta v_{dc})(\delta v_{LO}) \rangle_P$ is always near 100 percent between steps whenever $\Gamma < 0.1$. These effects show that the mixer characteristics are strongly influenced by the nonlinear interaction of noise.

Once the functions $\langle v_{dc} \rangle = f(i_{dc}, i_{LO})$ and $\langle v_{LO} \rangle = g_1(i_{dc}, i_{LO}) + j g_2(i_{dc}, i_{LO})$ are evaluated under various bias conditions, one can compute the modified I-V curves for a finite source impedance Z_{LO}. The load equations for the circuit on the left of Fig. 1 are

$$f(i_{dc}, i_{LO}) + r_{dc} i_{dc} = v_{S,dc} \tag{17}$$

$$g_1(i_{dc}, i_{LO}) + j g_2(i_{dc}, i_{LO}) + z_{LO} i_{LO} = v_{S,LO} = |v_{S,LO}| e^{j\theta} \tag{18}$$

where $r_{dc} = R_{dc}/R$, $z_{LO} = Z_{LO}/R$, and $v_{S,dc}$, $v_{S,LO}$ are normalized with respect to RI_c. For convenience, the phase angle θ of the LO generator is adjusted such that i_{LO} is real. Given r_{dc}, z_{LO}, $|v_{S,LO}|$, and $v_{S,dc}$, the algebraic equations (17), (18) can be solved graphically for θ, i_{dc}, i_{LO}, and, therefore $\langle v_{dc} \rangle = f(i_{dc}, i_{LO})$. The provides a point for the I-V curve. At a fixed LO power (constant $|v_{S,LO}|$), the entire I-V curve can be generated by repeating the process with different values of $v_{S,dc}$. The source resistance r_{dc} does not affect the shape of the I-V curve except for stability when there is a region of negative slope. Shown in Fig. 3 are two families of I-V curves computed at various LO power levels for two values of z_{LO}. The deviations from the well-known constant current case (inset) are obvious. They are in good agreement with experimental curves and analog simulator results [9]. When the RF termination is inductive as in Fig. 3(a), the current i_{LO} increases with dc bias between steps, resulting in a negative differential resistance. It can be stably biased only if r_{dc}^{-1} is larger than the magnitude of the slope. On the other hand, if the RF termination is capacitive as in Fig. 3(b), i_{LO} decreases as the bias voltage is increased. In this case, the dynamic resistance between steps becomes much lower, and the first step is reduced appreciably.

IV. Conversion and Noise-Correlation Matrices

Now we consider the mixer response to a small applied signal at a normalized frequency $\hbar\omega_u/2eRI_c = \Omega_u = \Omega_{LO} + \Omega_0$ (upper sideband or usb), where $\Omega_0 \ll \Omega_{LO}$. Based on the embedding circuit assumption, the current generated by the nonlinear Josephson element is only at intermediate frequency (IF) Ω_0 and image frequency $\Omega_l = \Omega_{LO} - \Omega_0$ (lower sideband or lsb), as shown on the right of Fig. 1. The small-signal current is then

$$i_{ss}(\tau) = (i_u e^{j\Omega_u \tau} + i_u^* e^{-j\Omega_u \tau}) + (i_0 e^{j\Omega_0 \tau} + i_0^* e^{-j\Omega_0 \tau}) + (i_l e^{j\Omega_l \tau} + i_l^* e^{-j\Omega_l \tau}) \tag{19}$$

in normalized units. If we add $i_{ss}(\tau)$ to (5) as a perturbation, the additional voltage (normalized) $d\phi_{ss}(\tau)/d\tau$ can be written

as

$$v_{ss}(\tau) = (v_u e^{j\Omega_u \tau} + v_u^* e^{-j\Omega_u \tau}) + (v_0 e^{j\Omega_0 \tau} + v_0^* e^{-j\Omega_0 \tau}) + (v_l e^{j\Omega_l \tau} + v_l^* e^{-j\Omega_l \tau}) + (\text{higher sidebands}). \quad (20)$$

Again we may ignore higher sideband voltage at $(2\Omega_{LO} \pm \Omega_0), \cdots$, etc. There are, of course, noise components at frequencies Ω_u, Ω_0, and Ω_l arising from fluctuations δv_{dc} and δv_{LO}. In the small-signal limit, the relationship between $v_{ss}(\tau)$ and $i_{ss}(\tau)$ is linear and can be described by a 3 × 3 impedance matrix

$$\begin{bmatrix} v_u \\ v_0 \\ v_l^* \end{bmatrix} = \begin{bmatrix} z_{uu} & z_{u0} & z_{ul} \\ z_{0u} & z_{00} & z_{0l} \\ z_{lu} & z_{l0} & z_{ll} \end{bmatrix} \begin{bmatrix} i_u \\ i_0 \\ i_l^* \end{bmatrix} + (\text{noise}) \quad (21)$$

or

$$\tilde{v}_s = \tilde{\tilde{Z}} \cdot \tilde{i}_s + \delta \tilde{v}_s. \quad (22)$$

All the matrix elements are normalized with respect to R. Since the IF is much lower than signal frequency in practice, the matrix can be determined from the pump solutions $\langle v_{dc} \rangle = f(i_{dc}, i_{LO})$, $\langle v_{LO} \rangle = g_1(i_{dc}, i_{LO}) + jg_2(i_{dc}, i_{LO})$ and their derivatives following a generalized mixer theory [15]

$$z_{uu} = \frac{1}{2}\left(\frac{\partial \langle v_{LO} \rangle}{\partial i_{LO}} + \frac{\langle v_{LO} \rangle}{i_{LO}}\right) \quad \text{(RF dynamic impedance)} \quad (23)$$

$$z_{u0} = \frac{\partial \langle v_{LO} \rangle}{\partial i_{dc}} \quad \text{(up-conversion)} \quad (24)$$

$$z_{ul} = \frac{1}{2}\left(\frac{\partial \langle v_{LO} \rangle}{\partial i_{LO}} - \frac{\langle v_{LO} \rangle}{i_{LO}}\right) \quad \text{(image conversion)} \quad (25)$$

$$z_{0u} = \frac{1}{2}\frac{\partial \langle v_{dc} \rangle}{\partial i_{LO}} \quad \text{(down-conversion)} \quad (26)$$

$$z_{00} = \frac{\partial \langle v_{dc} \rangle}{\partial i_{dc}} \quad \text{(dc dynamic resistance)} \quad (27)$$

and

$$z_{0l} = z_{0u}, \quad z_{lu} = z_{ul}^*, \quad z_{l0} = z_{u0}^*, \quad z_{ll} = z_{uu}^* \quad (28)$$

from symmetry. The second row of the matrix is real since i_{LO} has a zero phase. In contrast to resistive mixers, the calculated conversion matrix of a Josephson mixer is neither reciprocal nor passive; therefore, conversion gain is possible.

The impedance matrix depends on the junction parameters Ω_{LO}, Γ, as well as on the bias parameters i_{dc}, i_{LO}. (Without loss of generality, the bias currents can be used as a set of independent parameters instead of the dc and LO generator voltages.) A typical case is shown in Fig. 4, where the dc and RF dynamic impedance and the down-conversion impedance z_{0u} are plotted versus dc bias. All but the RF resistance show a symmetric shape between the zeroth and first induced steps. The mixer should be biased halfway between the steps for a maximum z_{0u}. If the noise parameter Γ is less than 0.1, z_{0u} is proportional to z_{00} as expected from earlier calculations [7]. In addition, the maximum z_{00} and z_{0u} are found to vary as $\Gamma^{-1/2}$ at a fixed Ω_{LO} [10], as shown in Fig. 5. As $\Gamma \to 1$, however, down-conversion is much less effective because of severe noise rounding of the steps.

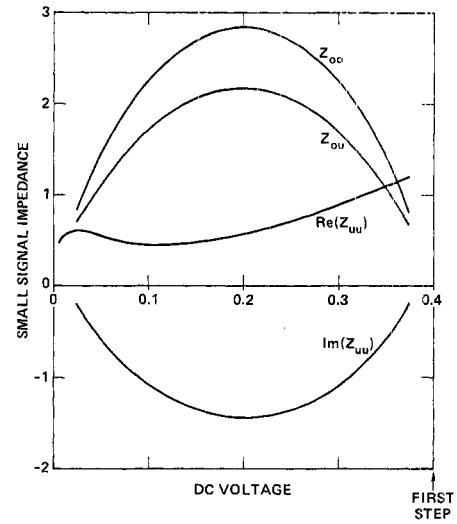

Fig. 4. Elements of the conversion matrix (normalized to R) as functions of bias voltage between the zeroth and first Josephson steps. They are computed for the same Ω_{LO}, Γ, and i_{LO} as those in Fig. 2, but for a more limited range of v_{dc}.

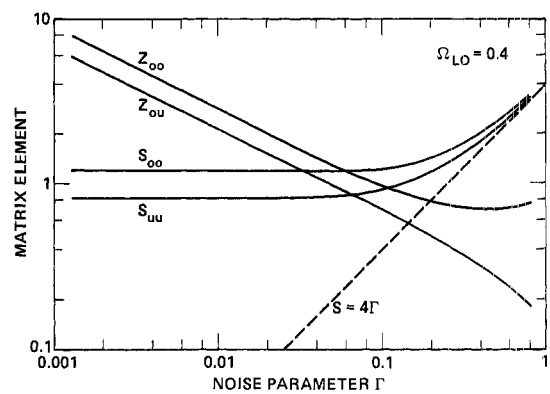

Fig. 5. Conversion and noise matrix elements versus noise parameter. All the quantities are taken at halfway between the first two steps, where the maximum values are insensitive to i_{LO}. The dashed line shows the spectral density of thermal noise without the ideal Josephson element.

In order to express the noise components in (21) explicitly, we consider a very-long observation time T (normalized) and expand δv_{dc}, δv_{LO} in Fourier series [16]

$$\delta v_{dc} = \sum_{n=-\infty}^{\infty} a_n e^{j(2n\pi/T)\tau}$$

$$\delta v_{LO} = \sum_{n=-\infty}^{\infty} b_n e^{j(2n\pi/T)\tau} \quad (29)$$

where $a_{-n} = a_n^*$ but $b_{-n} \neq b_n^*$. If a normalized bandwidth $\Delta f = 1/T$ is used for the mixer noise, we have

$$\tilde{\delta v}_s = \begin{bmatrix} b_N \\ a_N \\ b_{-N}^* \end{bmatrix} \quad (30)$$

for (22), where N satisfies $2\pi N/T = \Omega_0$. A noise correlation matrix can then be defined in terms of spectral densities

$$\tilde{\tilde{S}} = \begin{bmatrix} S_{uu} & S_{u0} & S_{ul} \\ S_{0u} & S_{00} & S_{0l} \\ S_{lu} & S_{l0} & S_{ll} \end{bmatrix} = 2T\langle(\tilde{\delta}v_s) \times (\tilde{\delta}v_s)^{T*}\rangle$$

$$= \begin{bmatrix} 2T\langle b_N b_N^*\rangle & 2T\langle b_N a_N^*\rangle & 2T\langle b_N b_{-N}\rangle \\ 2T\langle a_N b_N^*\rangle & 2T\langle a_N a_N^*\rangle & 2T\langle a_N b_{-N}\rangle \\ 2T\langle b_{-N}^* b_N^*\rangle & 2T\langle b_{-N}^* a_N^*\rangle & 2T\langle b_{-N}^* b_{-N}\rangle \end{bmatrix}. \quad (31)$$

Since the intermediate frequency Ω_0 is much smaller than Ω_{LO}, only the low-frequency spectra in (29) are of interest. In this case, the matrix $\tilde{\tilde{S}}$ can be evaluated from the auto- and crosscorrelations given by (13)–(16) [16]

$$S_{uu} = S_{ll} = 2P\langle|\delta v_{LO}|^2\rangle_P \quad (32)$$

$$S_{u0} = S_{0l} = S_{0u}^* = S_{l0}^* = 2P\langle(\delta v_{dc})(\delta v_{LO})\rangle_P \quad (33)$$

$$S_{ul} = S_{lu}^* = 2P\langle(\delta v_{LO})^2\rangle_P \quad (34)$$

$$S_{00} = 2P\langle(\delta v_{dc})^2\rangle_P. \quad (35)$$

The matrix $\tilde{\tilde{S}}$ is Hermitian and positive-definite with all the elements independent of P.

When the ac Josephson current is not synchronized, the noise spectral densities are much higher than that for thermal noise, $S = 4\Gamma$ (6), in the absence of nonlinear Josephson element. This is also shown in Fig. 5, where S_{00} and S_{uu} at halfway between the first two steps are plotted against the noise parameter Γ. There exists an analytic model for such an "excess" noise in the presence of a large LO current [17]. It gives an expression

$$S_{00} = 4\pi\langle v_{dc}\rangle(1 - \langle v_{dc}\rangle/\Omega_{LO}) \quad (36)$$

for $\langle v_{dc}\rangle$ between the zeroth and first steps. Similar to z_{0u}, S_{00} also has a maximum value ($=\pi\Omega_{LO}$) at $\langle v_{dc}\rangle = \Omega_{LO}/2$. Our computed results check out very well with (36) within the validity of the analytic theory in which $\Gamma < 0.1$. One notices that the voltage noise stays constant no matter how small the driving noise Γ is. This is consistent with the observed noise being much greater than thermal noise in a low-resistance, high critical-current junction [18]. The calculation also shows that the cross correlations given by the off-diagonal elements of $\tilde{\tilde{S}}$ are rather strong when $\Gamma \ll 1$ and $\Omega_{LO} < 1$.

V. Mixer Noise Temperature and its Optimization

Knowing the embedding circuit at signal, IF, and image frequencies, mixer conversion efficiency and noise temperature can be calculated from the conversion and noise correlation matrices [6]. The equations for the circuit on the right of Fig. 1 are

$$\begin{bmatrix} v_u \\ v_0 \\ v_l^* \end{bmatrix} + \begin{bmatrix} z_u & 0 & 0 \\ 0 & z_0 & 0 \\ 0 & 0 & z_l^* \end{bmatrix} \begin{bmatrix} i_u \\ i_0 \\ i_l^* \end{bmatrix} = \begin{bmatrix} v_{sig} \\ 0 \\ 0 \end{bmatrix} \quad (37)$$

or

$$\tilde{v}_s + \tilde{\tilde{Z}}_s \cdot \tilde{i}_s = \tilde{v}_{sig}. \quad (38)$$

Here $v_{sig} = V_{sig}/RI_c$, and z_u, z_0, z_l^* are normalized to R. Matrix equations (22) and (38) can be solved for the small-signal current

$$\tilde{i}_s = (\tilde{\tilde{Z}} + \tilde{\tilde{Z}}_s)^{-1} \cdot (\tilde{v}_{sig} - \tilde{\delta}v_s). \quad (39)$$

If we let

$$\tilde{\tilde{Y}} = (\tilde{\tilde{Z}} + \tilde{\tilde{Z}}_s)^{-1} = \begin{bmatrix} Y_{uu} & Y_{u0} & Y_{ul} \\ Y_{0u} & Y_{00} & Y_{0l} \\ Y_{lu} & Y_{l0} & Y_{ll} \end{bmatrix} \quad (40)$$

and

$$\tilde{Y}_0 = \begin{bmatrix} Y_{0u} \\ Y_{00} \\ Y_{0l} \end{bmatrix} \quad (41)$$

the IF current is simply given by the scalar equation

$$i_0 = \tilde{Y}_0^T \cdot (\tilde{v}_{sig} - \tilde{\delta}v_s) = Y_{0u}v_{sig} - \tilde{Y}_0^T \cdot \tilde{\delta}v_s. \quad (42)$$

The mean square IF current is, therefore,

$$2\langle i_0 i_0^*\rangle = 2|Y_{0u}|^2|v_{sig}|^2 + 2\tilde{Y}_0^T \cdot \langle(\tilde{\delta}v_s) \times (\tilde{\delta}v_s)^{T*}\rangle \cdot \tilde{Y}_0^*$$
$$= 2|Y_{0u}|^2|v_{sig}|^2 + (\tilde{Y}_0^T \cdot \tilde{\tilde{S}} \cdot \tilde{Y}_0^*)\Delta f. \quad (43)$$

Here (31) has been used for a noise bandwidth $\Delta f = 1/T$. Since the mixer conversion efficiency η is equal to the down-converted IF power divided by the available signal power, the signal term in (43) gives

$$\eta = \frac{2\,\mathrm{Re}\,(z_0)|Y_{0u}|^2|v_{sig}|^2}{2|v_{sig}|^2/4\,\mathrm{Re}\,(z_u)} = 4|Y_{0u}|^2\,\mathrm{Re}\,(z_u)\,\mathrm{Re}\,(z_0). \quad (44)$$

In order to obtain the mixer noise temperature T_M, we let the signal term equal the noise term in (43) and substitute $2|v_{sig}|^2$ with $4\,\mathrm{Re}\,(z_u)\Gamma_M\Delta f$ where $\Gamma_M = 2ekT_M/\hbar I_c$

$$\frac{T_M}{T} = \frac{\Gamma_M}{\Gamma} = \frac{(\tilde{Y}_0^T \cdot \tilde{\tilde{S}} \cdot \tilde{Y}_0^*)}{4\Gamma|Y_{0u}|^2\,\mathrm{Re}\,(z_u)}. \quad (45)$$

Another parameter of importance is the IF output impedance

$$z_{out} = Y_{00}^{-1} - z_0. \quad (46)$$

For a double-sideband (DSB) mixer, $z_u = z_l = z_{LO}$, it can be shown that z_{out} is real. For a single-sideband (SSB) mixer, $z_u \neq z_l$, and z_{out} is complex. In any case, z_{out} is independent of z_0. The IF load should, therefore, be conjugate matched for maximum conversion efficiency. That is, $z_0 = z_{out}^*$, provided that $\mathrm{Re}\,(z_{out}) > 0$. However, the output impedance may have a negative real part, such as the case in Fig. 3(a). Then the conversion efficiency is potentially unbounded. On the contrary, the mixer noise temperature is independent of z_0 and always remains finite and continuous. Therefore, it is the purpose of our optimization to find the minimum mixer noise temperature under a variety of conditions.

We first consider the dependence of T_M/T on RF impedance z_u, z_l for a given pair of matrices $\tilde{\tilde{Z}}$, $\tilde{\tilde{S}}$. An example is shown in Fig. 6, where constant T_M/T contours are plotted in a complex plane of signal impedance z_u. In both DSB and SSB

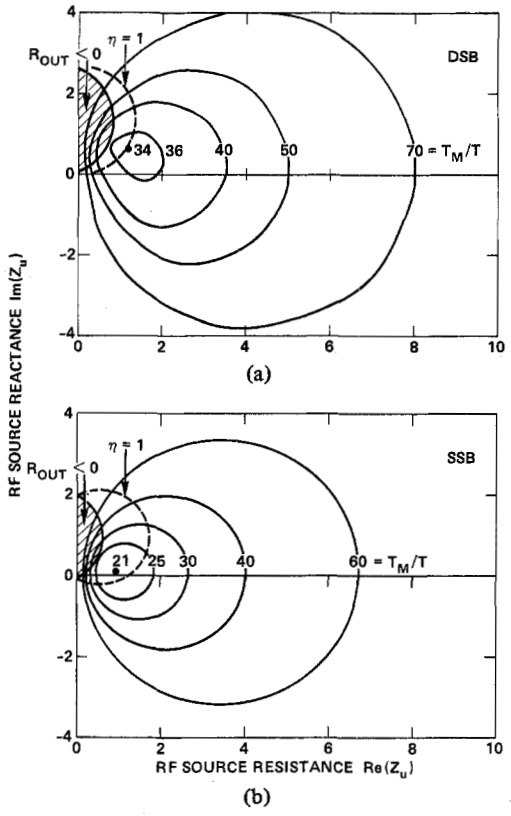

Fig. 6. Optimization of mixer noise temperature with respect to signal source impedance at a fixed bias, $\langle v_{dc} \rangle = 0.16$. Other parameters are the same as in Fig. 2. The dots indicate the signal impedances for minimum $T_M/T = 34$ (DSB) and $T_M/T = 21$ (SSB). For the SSB case in (b), the image impedance is fixed at its best value, $z_I = 4j$.

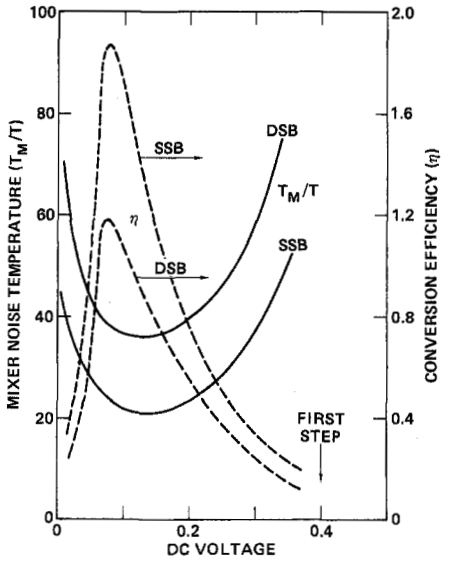

Fig. 7. Mixer noise temperature (solid curves) and corresponding conversion efficiency (dashed curves) versus dc bias. The optimum signal/image impedances for each bias are determined individually following a procedure similar to Fig. 6. The parameters $\Omega_{LO} = 0.4$, $\Gamma = 0.01$, $i_{LO} = 0.45$ are the same as in Fig. 2. At the bias voltage where T_M/T is lowest, the IF output impedances (normalized) are $z_{out} = 3.0$ for DSB, and $z_{out} = 1.0 + 1.6j$ for SSB.

cases,[1] minimum T_M/T takes place outside a shaded region of negative output resistance. Also shown in Fig. 6 are two dashed curves for unity conversion efficiency assuming a matched IF load. Stable conversion gain is obtained inside two moon-shape regions. The lowest noise temperature for SSB is appreciably better than that for DSB, since the image impedance z_I can be varied independently in the former case. The best image termination is always reactive and close to an open circuit. A short circuit at the image frequency usually results in a large noise temperature.

Optimization with respect to RF terminations is repeated for different matrices to obtain minimum T_M/T as a function of dc bias between the first two steps. A typical case is shown in Fig. 7, where the corresponding conversion efficiency is also plotted. Here the mixer is very noisy near either step, and the best bias is slightly below the voltage midway between the steps. In general, the bias voltage for maximum conversion efficiency does not coincide with that for lowest mixer noise temperature. Bias beyond the first Josephson step has also been explored, but the result is not as good. For a given junction (fixed Ω_{LO} and Γ), the minimum T_M/T is rather insensitive to LO current (i_{LO}), provided that a significant fraction of the zero-voltage current is suppressed by the LO power like the cases in Fig. 3. At a much higher LO power, however, the mixer performance does degrade.

The minimum T_M/T can be obtained under different optimum bias for a variety of junction parameters Γ and Ω_{LO}. The result is shown in Fig. 8 versus noise parameter Γ for two of the normalized frequencies studied. Also shown, in broken lines, are the corresponding conversion efficiencies. At a fixed normalized frequency, the mixer noise temperature divided by the ambient temperature is lowest around $\Gamma = 0.1$, where $\eta \approx 0.3$. It arises from two opposing effects: larger "excess" noise with respect to thermal noise at $\Gamma \ll 1$, and severe noise saturation when $\Gamma \to 1$. Such a minimum figure of T_M/T improves significantly toward lower values of Ω_{LO}. In particular, the theory predicts that a mixer noise temperature as low as five times the ambient temperature can be achieved in an SSB mixer at $\Omega_{LO} = 0.2$.

The sensitivity of a millimeter-wave heterodyne receiver is limited not only by the noise in the mixer but also by the noise in the following IF amplifier. The total receiver noise temperature with respect to the ambient temperature is

$$T_R/T = T_M/T + (1/\eta)(T_A/T) \tag{47}$$

where T_A is the amplifier noise temperature. Its contribution depends on the value of conversion efficiency. Since minimum T_M/T does not take place at maximum η, one must carry out the optimization for T_R/T also. Assuming a T_A/T equal to 5, which can be achieved by a cooled FET amplifier when $T \approx 4$ K, we obtain minimum receiver noise contours in an Ω_{LO}-Γ plane as shown in Fig. 9. The results are calculated for DSB and SSB receivers under the restriction $\mathrm{Re}(z_{out}) > 0$ and with a matched IF load. For a fixed normalized frequency, lowest T_R/T is found at a noise parameter between 0.02 and 0.05. This is shifted from $\Gamma \approx 0.1$ for minimum T_M/T toward a higher conversion efficiency. A comparison

[1]The terms DSB and SSB used in this paper are referring only to the input terminations of the mixer or receiver. All the conversion efficiency and noise temperature are for the detection of a narrow-band signal on one side of the LO, rather than for the figures inferred from a broad-band radiometric measurement.

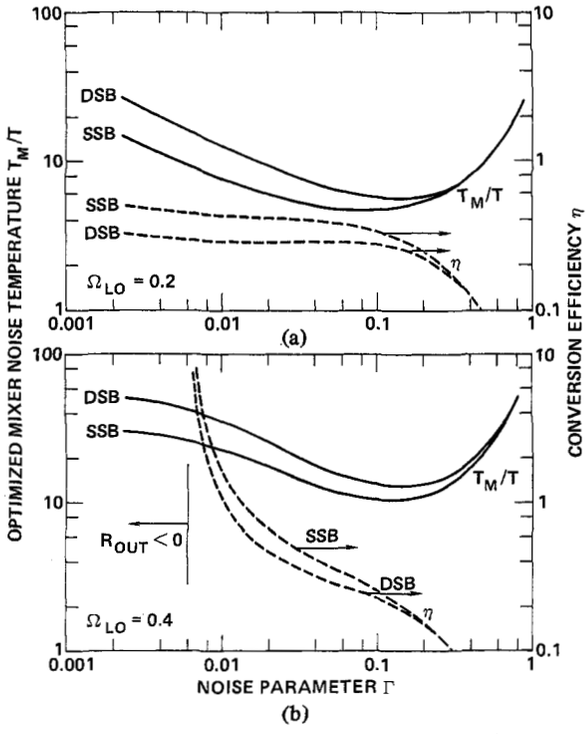

Fig. 8. DSB/SSB mixer noise temperature (solid) at best bias and corresponding conversion efficiency (dashed) versus noise parameter for two normalized frequencies shown. The output resistance becomes negative and η is unbounded below $\Gamma \equiv 2ekT/\hbar I_c \approx 0.006$ when $\Omega_{LO} \equiv \hbar\omega_{LO}/2eRI_c = 0.4$. There is no such divergence for $\Omega_{LO} = 0.2$ over the range of parameter studied.

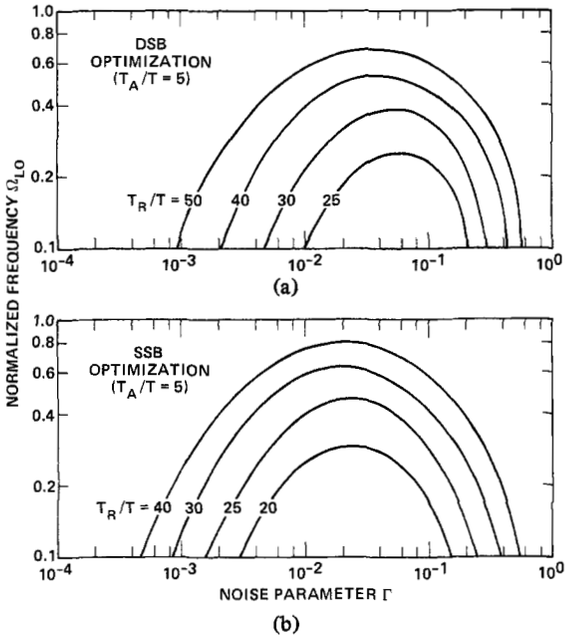

Fig. 9. Constant DSB and SSB receiver noise temperature contours in a plane of normalized frequency-noise parameter. Each number represents the best figure that can be achieved theoretically for a given junction. The IF output resistance is positive and matched throughout all cases. Here $\Gamma \equiv 2ekT/\hbar I_c$, and $\Omega_{LO} \equiv \hbar\omega_{LO}/2eRI_c$.

between Fig. 9(a) and (b) shows that an SSB receiver is better than a DSB receiver at the same Ω_{LO} and Γ by an average factor of one and a half. The prediction that an SSB Josephson receiver at $\Omega_{LO} = 0.2$ can have T_R/T less than 20 over a wide range of Γ is very encouraging.

VI. Discussion and Conclusion

Although there are fundamental differences between a Josephson mixer and a conventional resistive mixer, we have generalized the classical mixer theory in order to include such effects as conversion gain, negative resistance, noise saturation, and correlation. The analysis can be extended to other nonlinear Josephson devices as well. For example, we have examined a few cases for parametric amplification when the RF input impedance has a negative real part. The amplifier operates either with one idler at the image frequency or with two idlers at both the image and the difference frequencies. It is found that the noise temperature at a finite voltage is much worse than that of a mixer at the same bias. The range of parameters for such a parametric amplifier is also very restricted. Another device of interest is a harmonic mixer which can be studied following a similar approach.

Previous experimental data on millimeter-wave Josephson mixers [1]-[3] have shown a noise temperature $T_M/T = 20$-50 with a conversion efficiency $\eta = 0.5$-1.3 at a normalized frequency $\Omega_{LO} = 0.3$-0.4 and a noise parameter $\Gamma = 0.01$ or less. They are in good agreement with the computed results. The theory also predicts that significant improvement is possible if a hysteresis-free junction can be made with a low critical current and a moderately high RI_c product. Specifically, for an RI_c product equal to one-half of the niobium energy gap or 1 mV and an $I_c = 10\ \mu$A at $T = 4.2$ K, the noise temperature of an SSB Josephson receiver at 100 GHz would be as low as $T_R = 70$ K, provided that $T_A = 20$ K for the IF amplifier. A single-sideband configuration can be realized using a reactive narrow-band filter in front of the mixer. It has an additional advantage that the background noise contribution to the system is reduced by a factor of two.

In the beginning of the analysis, it is assumed that the spectral density of thermal noise is kT at all frequencies. The assumption breaks down in the quantum limit at a frequency higher than kT/h [10], or approximately 100 GHz at $T = 4.2$ K. In the limit when $\omega_{LO} \approx kT/\hbar$, the extra photon noise at frequencies beyond ω_{LO} does not have a very strong effect on the mixer since the noise components in Fig. 5 are practically independent of Γ. However, as the ambient temperature is reduced such that $kT \ll \hbar\omega_{LO}$, one can no longer expect T_M to improve with T. In order to explore such a transition into quantum limit, the noise term in (4) must satisfy a nonuniform spectrum for quantum fluctuations. This can be simulated in computer calculations with a series of properly correlated random numbers in the time domain.

In conclusion, we have carried out a complete numerical characterization as well as optimization for a Josephson-junction mixer. A nonlinear pump equation based on the RSJ model with thermal noise is solved in the time domain to obtain a conversion matrix and a noise correlation matrix. These matrices are then used in the frequency domain to calculate the noise temperature and conversion efficiency. Optimization is made in a multiparameter space to find the best mixer and receiver performance. The prediction from the analysis is very promising and may be realized using high-quality junctions.

ACKNOWLEDGMENT

The author would like to thank A. R. Kerr and J. H. Claassen for many fruitful discussions during the course of the work.

REFERENCES

[1] Y. Taur, J. H. Claassen, and P. L. Richards, "Conversion gain in a Josephson effect mixer," *Appl. Phys. Lett.*, vol. 24, pp. 101-103, Jan. 1974.
[2] J. H. Claassen and P. L. Richards," Point-contact Josephson mixers at 130 GHz," *J. Appl. Phys.*, vol. 49, pp. 4130-4140, July 1978.
[3] Y. Taur and A. R. Kerr, "Low-noise Josephson mixers at 115 GHz using recyclable point contacts," *Appl. Phys. Lett.*, vol. 32, pp. 775-777, June 1978.
[4] J. H. Claassen, Y. Taur, and P. L. Richards, "Noise in Josephson point contacts with and without RF bias," *Appl. Phys. Lett.*, vol. 25, pp. 759-761, Dec. 1974.
[5] Y. Taur, "Noise down-conversion in a pumped Josephson junction," *J. Phys.*, vol. 39-C6, pp. 575-576, Aug. 1978.
[6] D. N. Held and A. R. Kerr, "Conversion loss and noise of microwave and millimeter-wave mixers: Part 1-Theory," *IEEE Trans. Microwave Theory Tech.*, vol. MTT-26, pp. 49-55, Feb. 1978.
[7] F. Auracher and T. Van Duzer, "Numerical calculations of mixing with superconducting weak links," in *Proc. Appl. Superconductivity Conf.*, pp. 603-607, Sept. 1972.
[8] Y. Taur, "Josephson junctions as microwave heterodyne detectors," Ph.D dissertation, University of California, Berkeley, 1974.
[9] Y. Taur, J. H. Claassen, and P. L. Richards, "Conversion gain and noise in a Josephson mixer," *Rev. Phys. Appl.*, vol. 9, pp. 263-268, Jan. 1974.
[10] J. H. Claassen and P. L. Richards, "Performance limits of a Josephson-junction mixer," *J. Appl. Phys.*, vol. 49, pp. 4117-4129, July 1978.
[11] Y. Taur, P. L. Richards, and F. Auracher, "Application of the shunted junction model to point-contact Josephson junctions," in *Proc. 13th Conf. Low Temp. Phys.*, vol. 3, pp. 276-280, Aug. 1972.
[12] B. D. Josephson, "Possible new effects in superconductive tunneling," *Phys. Lett.*, vol. 1, pp. 251-253, July 1962.
[13] A. R. Kerr, private communication.
[14] F. Auracher and T. Van Duzer, "RF impedance of superconducting weak links," *J. Appl. Phys.*, vol. 44, pp. 848-851, Feb. 1973.
[15] H. C. Torrey and C. A. Whitmer, *Crystal Rectifiers.* New York: McGraw-Hill Book, 1948, ch. 5.
[16] A. Van der Ziel, *Noise; Sources, Characterization, Measurement.* Englewood Cliffs, NJ: Prentice-Hall, 1970, ch. 2.
[17] D. W. Peterson and Y. Taur, to be published.
[18] D. W. Peterson, "The unclamped and current clamped SUPAR-AMP: Studies of the unbiased Josephson junction parametric amplifier," Ph.D dissertation, University of California, Berkeley, 1978.

Externally Pumped Millimeter-Wave Josephson-Junction Parametric Amplifier

M. T. LEVINSEN, NIELS F. PEDERSEN, OLE H. SOERENSEN, BENNY DUEHOLM, AND JESPER MYGIND

Abstract—**A unified theory of the singly and doubly degenerate Josephson-junction parametric amplifier is presented. Experiments with single junctions on both amplifier modes at frequencies 10, 35, and 70 GHz are discussed. Low-noise temperature (~100 K, single sideband (SSB)) and reasonable gain (~8 dB) were obtained at 35 GHz in the singly degenerate mode. On the basis of the theory and experiments, a general procedure for optimizing junction parameters is discussed and illustrated by the specific design of a 100-GHz amplifier.**

Manuscript received February 5, 1980; revised June 16, 1980. This work was supported in part by the Danish Natural Science Research Council under Grants 511-5616, 511-8527, 511-10098, 511-10279, 511-15159, and 511-20013.

M. T. Levinsen is with Physics Laboratory I, H. C. Ørsted Institute, DK-2100 Copenhagen, Denmark.
N. F. Pedersen, O. H. Soerensen, B. Dueholm, and J. Mygind are with Physics Laboratory I, Technical University of Denmark, DK-2800 Lyngby, Denmark.

I. INTRODUCTION

PARAMETRIC AMPLIFICATION based on external modulation of the nonlinear Josephson inductance has been studied for almost a decade [1]-[14]. The efforts have been devoted mainly to two different single-idler modes. The doubly degenerate amplifier (DDA) first suggested by Parrish *et al.* [1] uses a single matching circuit centered at the pump frequency f_p. The dominant idler is at the frequency $f_i = 2f_p - f_s$, where f_s is the signal frequency. In the DDA maximum gain occurs at $f_s \simeq f_i \simeq f_p$. It has been standard to operate the DDA at zero dc-bias current where the nonlinearity is of second order (the leading term of the Josephson inductance is at $2f_p$). The doubly degenerate mode has been thoroughly studied at *X* band by Feldman *et al.* [2], and by Wahlsten *et al.* [3], and at *Ka* band by Taur and Richards [4], and Goodall *et al.* [5].

0018/9383/80/1000-1928$00.75